MEMO

Date: October 23, 2009
To: Jason Cotrell and Scott Lambert
From: Jason Jonkman
Re: Non-Torque Load (NTL) Specifications for the NWTC Dynamometer Upgrade

On October 12, 2009, Jason Cotrell asked me to comment on the expected load range and frequency content required to accurately capture NTLs in the NWTC dynamometer upgrade. The NTLs of interest are the shear forces, bending moments, and thrust in the low-speed shaft. To address this request, I reprocessed the outputs of an analysis I performed earlier on the conceptual land-based NREL 5-MW baseline wind turbine, which is a conventional three-bladed upwind variable-speed, variable blade-pitch-to-feather-controlled turbine derived from representative specifications of real and conceptual 5-MW turbines [1]. A comprehensive loads analysis for this turbine was performed with the FAST aero-servo-elastic simulation tool, using the International Electrotechnical Commission (IEC) 61400-series design standards as a guide, as presented in Ref. [2].

The drivetrain loads for the NREL 5-MW turbine—as presented in Ref. [2]—are given in terms of statistics, time series, and extreme event tables. Additionally—as presented in Ref. [3]—the drivetrain fatigue loads are given in terms of damage-equivalent loads (DELs). Moreover, these loads were all calculated in the low-speed shaft (LSS) at the main bearing in a coordinate system that rotates with the shaft. Because the NTLs in the NWTC dynamometer upgrade will be applied in a fixed frame, for the purposes of the present analysis, the drivetrain load time series from Ref. [2] have been transformed to the nonrotating frame (i.e., in a coordinate system fixed in the nacelle). To estimate the load ranges, the statistics (minimum, mean, maximum, and standard deviation) of the transformed time series are calculated. Furthermore, to estimate the frequency content, the one-sided power-spectral densities (PSDs) and the square root of the one-sided cumulative-spectral densities (CSDs) of the transformed time series are also calculated.[1] These calculations are run from three representative simulations of normal operation under normal turbulence: one near, one below, and one above rated wind speed. As shown in Refs. [2] and [3], the ultimate and fatigue loads in the drivetrain of the NREL 5-MW turbine are dominated by normal operation under normal and extreme turbulence. So, the present results are meant to be *representative*, not conservative. The PSD and CSD calculations are explained in this Memo's Appendix.

[1] A PSD and CSD characterize how the power of a time series is distributed with frequency. The square root of the high-frequency limit of the CSD—that is, $\sigma_x(\infty)$, where $\sigma_x()$ is defined in this Memo's Appendix—equals the standard deviation of the time series.

In the parameter names of the presented results, "LSSGag" represents the LSS load (strain) gage, which is a node placed in the shaft at the main bearing used for tracking drivetrain loads in FAST; "F" represents a force; "M" represents a moment; and "xs," "ys," and "zs" represent the axes of the nonrotating shaft coordinate system, where the xs-axis is along the shaft in the (nominally) downwind direction, the ys-axis is pointed to the left when looking (nominally) downwind, and the zs-axis is pointed up (nominally opposite gravity). For example, "LSSGagFxs" represents the axial (thrust) force and "LSSGagMys" represents the horizontal bending moment transmitted through the LSS at the main bearing. The drivetrain loads presented are not scaled by any safety factors.

The statistical results at 12 m/s (near rated wind speed) are presented in Table I. These results were calculated by reprocessing the output of the simulation named DLC1.1_0025_Land_12.0V0_S01.out from Ref. [2]. The mean rotor thrust and torque are 675.1 kN and 3884.5 kN·m, respectively. The mean vertical shear force and horizontal bending moment are -1078.5 kN and -1397.5 kN·m, respectively, which are caused primarily by the overhanging weight of the rotor. The horizontal shear force and vertical bending moment—perhaps, surprisingly—have nonzero means (of -5.1 kN and 501.8 kN·m, respectively). These means are due to a nonzero mean lateral deflection of the tower induced by the rotor torque. The deviations about these means are due to turbulence in the wind inflow and the resulting variations in aerodynamic loads and structural motions.

Table I. Statistics at 12 m/s

	LSSGagFxs	LSSGagFys	LSSGagFzs	LSSGagMxs	LSSGagMys	LSSGagMzs
	kN	kN	kN	kN·m	kN·m	kN·m
min	411.3	-56.8	-1140.7	2556.0	-6336.2	-3879.7
mean	675.1	-5.1	-1078.5	3884.5	-1397.5	501.8
max	920.1	51.4	-1017.2	4627.0	2699.9	5180.7
stddev	107.1	14.5	15.7	443.7	1338.6	1283.8

The spectral results at 12 m/s (from DLC1.1_0025_Land_12.0V0_S01.out) are plotted in Figure 1. The mean rotor speed at this wind condition is about 11.9 rpm, which translates to a once-per revolution (1P) frequency of about 0.2 Hz. The corresponding three-per revolution (3P), 6P, and 9P frequencies are at about 0.6 Hz, 1.2 Hz, and 1.8 Hz, respectively. All of the drivetrain loads clearly show excitation at 3P, 6P, and 9P. The shear forces, furthermore, show excitation at 1P, which is induced by a slight mass imbalance in the rotor (representing manufacturing variations). Additional excitation is visible in the shear forces (particularly the side-to-side shear force) at about 0.32 Hz, which corresponds with the 1st bending fore-aft and side-to-side bending modes of the tower. The spikes at zero frequency indicate the nonzero mean loads. A lot of excitation

also occurs just above zero frequency, which is where the turbulent energy is the highest. As expected, the high-frequency limits of the square root of the CSDs correspond with the standard deviations of the time series from Table I. However, most of the power in all loads is captured in the frequencies between zero and 3P.

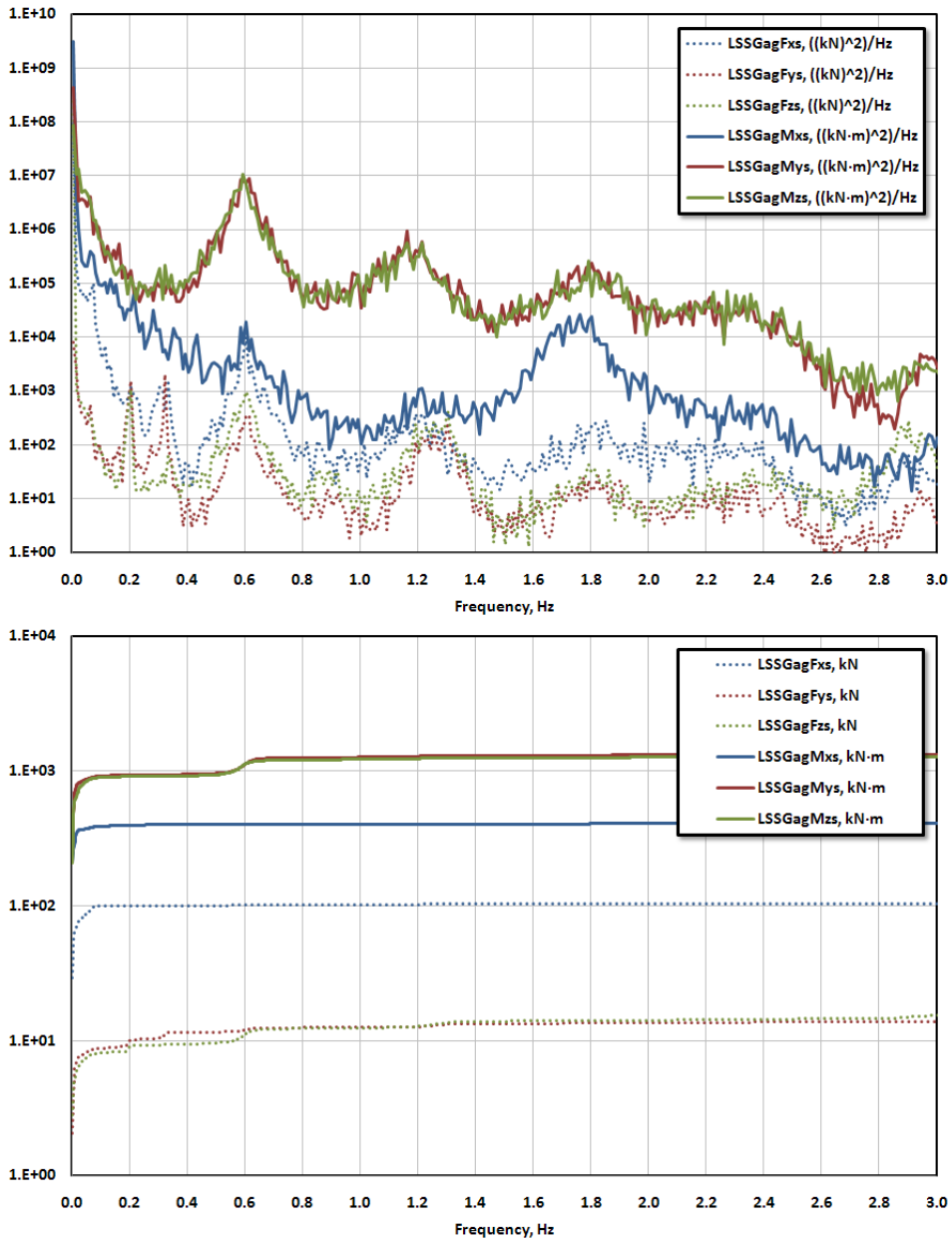

Figure 1. PSDs (left) and square roots of the CSDs (right) at 12 m/s

The results at 8 m/s (midway between cut-in and rated wind speeds) are presented in Table II and Figure 2 and the results at 18 m/s (midway between rated and cut-out wind speeds) are presented in Table III and Figure 3. These results were calculated by reprocessing the output of the simulations named DLC1.1_0013_Land_08.0V0_S01.out and DLC1.1_0043_Land_18.0V0_S01.out from Ref. [2], respectively. When compared with the results at 12 m/s, as expected, the thrust is highest near rated wind speed and the torque increases with wind speed. The increase in torque with wind speed causes the horizontal shear force and vertical bending moment also to increase with wind speed. The drivetrain load standard deviations increase with wind speed in most components due to the increased standard deviation in the wind-inflow turbulence with wind speed. The mean rotor speed at 18 m/s is, as expected, equal to the rated rotor speed of 12.1 rpm, which translates to similar 1P, 3P, 6P, and 9P frequencies as were at 12 m/s. But at 8 m/s, the mean rotor speed drops to about 9.2 rpm, which translates to 1P, 3P, 6P, and 9P frequencies of about 0.153, 0.46 Hz, 0.92 Hz, and 1.38 Hz, respectively. The excitations in the drivetrain loads near zero frequency, 1P (for shear), 3P, and 6P are clearly visible at 8 m/s and 18 m/s, just as they were at 12 m/s. The 9P excitations, however, are less noticeable at 8 m/s and 18 m/s than they were at 12 m/s. At 8 m/s, the rotor torque is shown to be excited at about 1.72 Hz, which corresponds with the natural frequency of the free-free drivetrain torsion mode (influenced by blade edgewise flexibility; the frequency would be closer to 2.2 Hz if the rotor were rigid). This torque excitation is less noticeable at 12 m/s and 18 m/s because of the torsional frequency's close proximity with the 9P frequency. As at 12 m/s, most of the power in all loads at 8 m/s and 18 m/s is captured in the frequencies between zero and 3P.

Table II. Statistics at 8 m/s

	LSSGagFxs	LSSGagFys	LSSGagFzs	LSSGagMxs	LSSGagMys	LSSGagMzs
	kN	kN	kN	kN·m	kN·m	kN·m
min	281.7	-34.2	-1112.7	933.6	-5590.6	-3381.9
mean	472.5	-3.3	-1075.5	1933.1	-1827.4	218.3
max	759.8	30.1	-1039.7	3359.0	1413.2	3334.2
stddev	75.5	9.3	9.2	405.4	1048.0	985.4

Table III. Statistics at 18 m/s

	LSSGagFxs	LSSGagFys	LSSGagFzs	LSSGagMxs	LSSGagMys	LSSGagMzs
	kN	kN	kN	kN·m	kN·m	kN·m
min	208.0	-123.1	-1157.0	3360.0	-7360.2	-5374.1
mean	444.8	-15.8	-1072.6	4181.5	-923.9	248.7
max	831.3	67.7	-986.8	4980.0	5607.7	7189.8
stddev	78.7	23.2	24.4	203.7	1673.1	1756.9

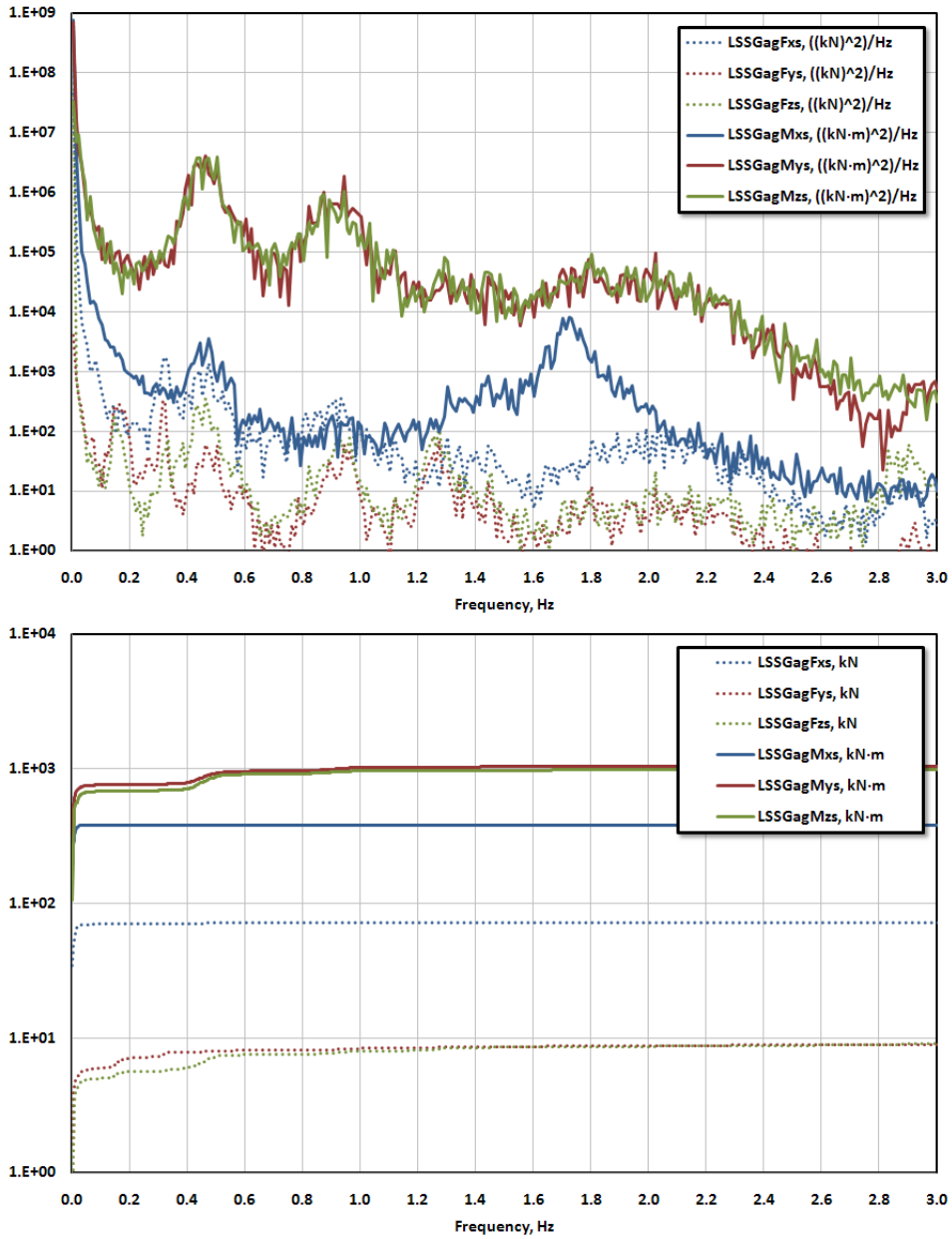

Figure 2. PSDs (left) and square roots of the CSDs (right) at 8 m/s

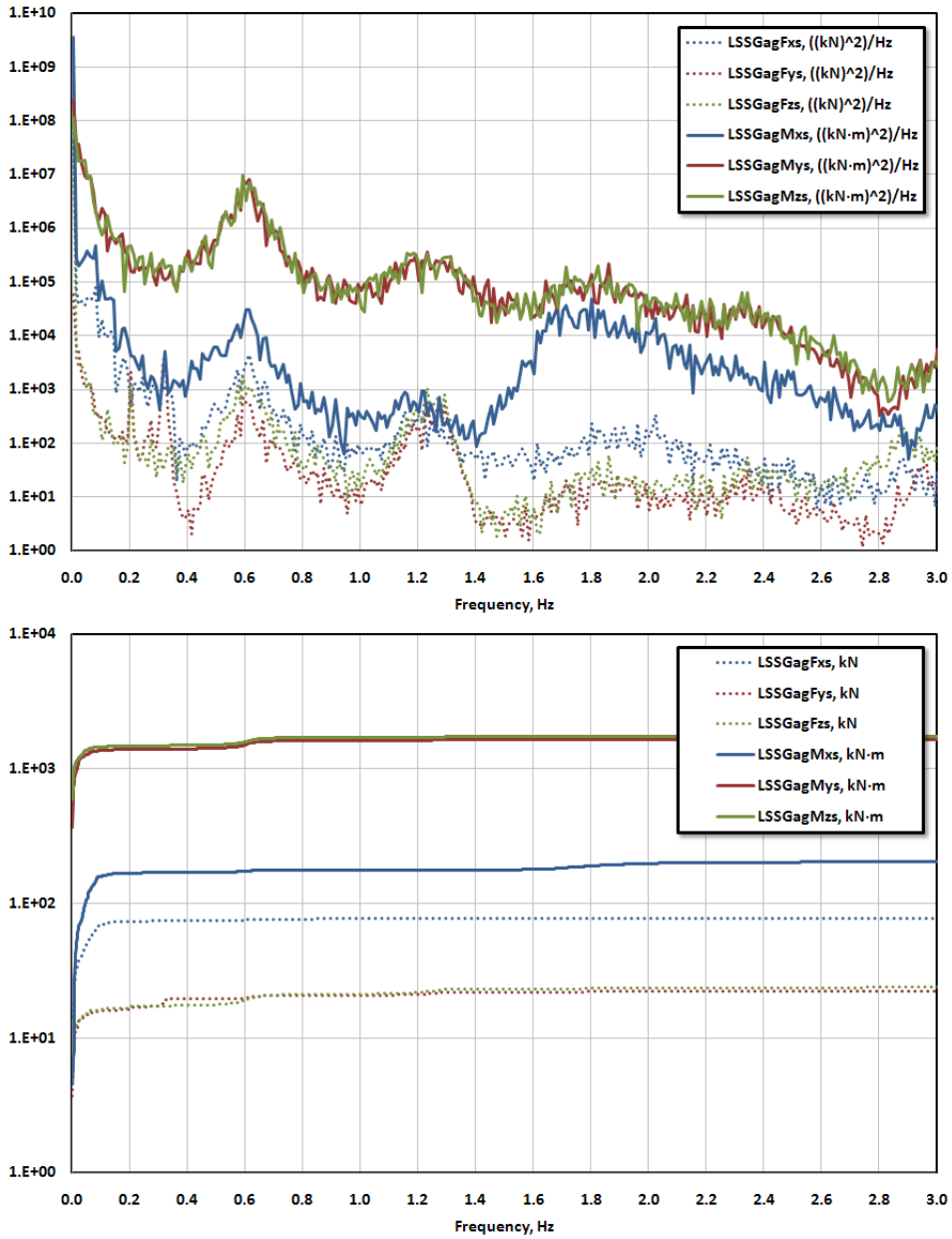

Figure 3. PSDs (left) and square roots of the CSDs (right) at 18 m/s

The highest loads presented in Table I through Table III are not the overall ultimate loads expected in the drivetrain, because—as stated above—the results presented above are just meant to be representative. The overall ultimate loads in the drivetrain must be found by processing all of loads from a comprehensive loads analysis, taking into account variations in wind and operational conditions, as well as applying partial safety factors

for loads. Such loads were identified for the NREL 5-MW wind turbine in Ref. [2] in the form of extreme-event tables. The extreme-event table for the drivetrain loads from Ref. [2] is represented in Table IV. The extreme-event tables record

- The extreme minimum and maximum loads (the shaded values on the block diagonal) for each load (identified in the first column)
- The name of the simulation that triggered the extreme load (third column)
- The associated values of the other parameters that occur when the extreme load is reached (off-diagonal values).

Table IV. Extreme Drivetrain Loads

Parameter	Type	File	LSSGagFxs kN	LSSGagFMyz kN	LSSGagMxs kN·m	LSSGagMMyz kN·m
LSSGagFxs	min	DLC1.4_0002_Land_ECD+R.out	-10.9	1470.0	4520.0	6400.0
LSSGagFxs	max	DLC1.3_0051_Land_20.0V0_S03.out	1530.0	1430.0	5900.0	2900.0
LSSGagFMyz	min	DLC1.3_0062_Land_24.0V0_S02.out	408.0	1150.0	5400.0	8980.0
LSSGagFMyz	max	DLC1.1_0063_Land_24.0V0_S03.out	706.0	1830.0	6380.0	10000.0
LSSGagMxs	min	DLC1.3_0003_Land_04.0V0_S03.out	104.0	1460.0	-73.6	4610.0
LSSGagMxs	max	DLC1.1_0062_Land_24.0V0_S02.out	875.0	1590.0	7840.0	2810.0
LSSGagMMyz	min	DLC1.1_0056_Land_22.0V0_S02.out	519.0	1630.0	6140.0	-28.5
LSSGagMMyz	max	DLC1.4_0002_Land_ECD+R.out	1100.0	1370.0	5640.0	15700.0

In Table IV, the horizontal and vertical shear forces and bending moments have been replaced with the magnitudes of the shear force vector and bending moment vector in the ys- and zs- plane [the vector magnitudes do not depend on the frame (rotating or nonrotating)]. The overall ultimate loads from Table IV are over 50% higher than the highest loads from Table I through Table III.

The final load range and frequency content required to accurately capture NTLs in the NWTC dynamometer upgrade should be up to the decision of the design team. The results presented above should provide adequate guidance to make proper design decisions.

Sincerely,

Jason

Jason Jonkman, Ph.D.
National Wind Technology Center (NWTC)
National Renewable Energy Laboratory (NREL)
1617 Cole Blvd.
Golden, CO. 80401-3393

Phone: +1 (303) 384 – 7026
Fax: +1 (303) 384 – 6901
E-mail: jason.jonkman@nrel.gov

References:

[1] Jonkman, J., Butterfield, S., Musial, W., and Scott, G., *Definition of a 5-MW Reference Wind Turbine for Offshore System Development*, NREL/TP-500-38060, Golden, CO: NREL, February 2009.

[2] Jonkman, J. M., *Dynamics Modeling and Loads Analysis of an Offshore Floating Wind Turbine*, Ph.D. Thesis, Department of Aerospace Engineering Sciences, University of Colorado, Boulder, CO, 2007; NREL/TP-500-41958, Golden, CO: NREL.

[3] Matha D, *Model Development and Loads Analysis of an Offshore Wind Turbine on a Tension Leg Platform, with a Comparison to Other Floating Turbine Concepts*, M.S. Thesis, SWE, University of Stuttgart, Germany, 2009; NREL/TP-500-45891, Golden, CO: NREL.

Appendix:

In the present analysis, the raw one-sided PSDs (see Eq. 1) are calculated directly by discrete-time Fourier transform (DFT) (see Eq. 2) without detrending or windowing of the time series. But to minimize scatter, the PSD results are binned into 0.01 Hz bins. The DFT, in turn, is calculated using an FFT algorithm. The square-roots of the one-sided CSDs (see Eq. 3) are calculated by numerical integration of the raw PSDs.

$$S_x(f)\Big|_{f=k\Delta f} = \frac{2}{\Delta f}\left(\frac{X[k]}{N}\right)\left(\frac{X[k]}{N}\right)^* \quad for\ k = 0,1,\ldots,\frac{N}{2}-1 \qquad \text{(Eq. 1)}$$

$$X[k] = \sum_{n=0}^{N-1} x(t)\Big|_{t=n\Delta t} e^{-j\frac{2\pi k n}{N}} \quad for\ k = -\frac{N}{2}+1, -\frac{N}{2}+2, \ldots, \frac{N}{2} \qquad \text{(Eq. 2)}$$

$$\sigma_x(f) = \sqrt{\int_0^f S_x(f')df'} \qquad \text{(Eq. 3)}$$

The $()^*$ in Eq. 1 represents the complex conjugate. Equations 1-3 use the following variable definitions:
$x()$ = continuous-time series

$S_x()$= one-sided PSD of x, defined in Eq. 1
$X[]$ = DFT of x, defined in Eq. 2
$\sigma_x()$= square-root of the one-sided CSD of x, defined in Eq. 3
n = discrete-time-step counter
k = discrete-frequency-step counter
N = number of discrete steps, $N = \frac{t_{max}}{\Delta t} = \frac{2 f_{max}}{\Delta f} = \frac{1}{\Delta t \Delta f}$ by the sampling theorem
t = time
t_{max}= maximum time
Δt = discrete-time step
f' = dummy frequency
f = frequency
f_{max}= maximum frequency
Δf = discrete-frequency step
j = imaginary number, $j = \sqrt{-1}$